Synthesis of Calcite Single Crystals with Porous Surface by Templating of Polymer Latex Particles

Conghua Lu, Limin Qi,* Hailin Cong, Xiaoyu Wang, Jinhu Yang, Linglu Yang, Dayong Zhang, Jiming Ma, and Weixiao Cao

State Key Laboratory for Structural Chemistry of Unstable and Stable Species, College of Chemistry, Peking University, Beijing 100871, P. R. China

Monodispersed copolymer latex particles functionalized by surface carboxylate groups are used as effective colloidal templates for the controlled crystallization of calcium carbonate in solution. After template removal, well-defined, calcite single crystals exhibiting a rhombohedral morphology and uniform surface pores are obtained. The surface pore size of the calcite single crystals can be readily adjusted through introduction of latex particles with varied sizes. The effects of the surface functional groups of the latexes, the concentration of the latex dispersion and $CaCl_2$ solution and the temperature during the $CaCO_3$ crystallization have been investigated. A three-step mechanism has been proposed for the formation of the composite particles consisting of calcite single crystals and latex particles, and it has been demonstrated that this synthesis strategy is potentially extendable to the synthesis of regularly shaped composite particles consisting of single crystals of other inorganic materials, such as Cu_2O. In addition, surface-patterned calcite crystals with hierarchical architectures are prepared at a relatively high concentration of latex particles, which act as both colloidal templates and crystal growth modifiers.

Introduction

The development of bottom-up crystallization strategies to fabricate single crystals patterned at the micro- and nanoscale remains an attractive challenge since these patterned structures are useful materials in various technological fields and important components in electronic, optical, and sensory devices.[1] It is well-known that biological organisms produce a wide variety of micropatterned biominerals with intricate and fascinating architectures through the elaborate biomineralization process.[2] For example, echinoderms, such as sea urchin and brittle stars, form skeletal parts consisting of micropatterned calcite single crystals that show delicate fenestrated structures and fulfill different functions.[3] Inspired by biominerals, the biomimetic synthesis of patterned inorganic materials is attracting increasing interest. In particular, the morphosynthesis of calcium carbonate, which is one of the most abundant biominerals and exhibits rather rich polymorphs, including calcite, aragonite, vaterite, and amorphous calcium carbonate, has received considerable attention.[4] Morphology-controlled synthesis of $CaCO_3$ crystals has been achieved in the presence of different soluble additives[5] and a variety of organized assemblies or soft templates.[6] Moreover, mercaptobenzoic acid-capped Au nanoparticles have been used as nucleation templates[7a] for

the controlled growth of vaterite and aragonite crystals, while calcium phosphotungstate nanoparticles have been employed as templates for the growth of star-shaped calcite crystal assemblies.[7b] On the other hand, patterned polycrystalline calcite thin films have been synthesized by using polysaccharide thin films,[8a] and self-assembled monolayers[8b] and multilayers[8c] as templates or through amorphous-to-crystalline transition on a solid substrate.[8d] Notably, there have been a few reports on the fabrication of porous $CaCO_3$ single crystals; examples include micropatterned calcite single crystals produced through amorphous-to-crystalline transition on micropatterned templates,[1] spongelike calcite single-

* Corresponding author. E-mail: liminqi@pku.edu.cn.

(1) Aizenberg, J.; Muller, D. A.; Grazul, J. L.; Hamann, D. R. *Science* **2003,** *299,* 1205.
(2) (a) Mann, S. *Biomineralization: principles and concepts in bioinorganic materials chemistry*; Oxford University Presss: New York, 2001. (b) Mann, S. *Angew. Chem., Int. Ed.* **2000,** *39,* 3392.
(3) Politi, Y.; Arad, T.; Klein, E.; Weiner, S.; Addadi, L. *Science* **2004,** *306,* 1161.
(4) (a) Kato, T.; Sugawara, A.; Hosoda, N. *Adv. Mater.* **2002,** *14,* 869. (b) Cölfen, H. *Curr. Opin. Colloid Interface Sci.* **2003,** *8,* 23.

(5) (a) Cölfen, H.; Qi, L. *Chem. Eur. J.* **2001,** *7,* 106. (b) Donners, J.; Nolte, R.; Sommerdijk, N. *J. Am. Chem. Soc.* **2002,** *124,* 9700. (c) Imai, H.; Terada, T.; Yamabi, S. *Chem. Commun.* **2003,** 484. (d) Estroff, L. A.; Incarvito, C. D.; Hamilton, A. D. *J. Am. Chem. Soc.* **2004,** *126,* 2. (e) Mukkamala, S. B.; Powell, A. K. *Chem. Commun.* **2004,** 918. (f) Euliss, L. E.; Trnka, T. M.; Deming, T. J.; Stucky, G. D. *Chem. Commun.* **2004,** 1736. (g) Volkmer, D.; Fricke, M.; Huber, T.; Sewald, N. *Chem. Commun.* **2004,** 1872. (h) Yu, J.; Yu, J. C.; Zhang, L.; Wang, X.; Wu, L. *Chem. Commun.* **2004,** 2414. (i) Wang, T.; Colfen, H.; Antonietti, M. *J. Am. Chem. Soc.* **2005,** *127,* 3246.
(6) (a) Qi, L.; Li, J.; Ma, J. *Adv. Mater.* **2002,** *14,* 300. (b) Yang, D.; Qi, L.; Ma, J. *Chem. Commun.* **2003,** 1180. (c) Li, M.; Mann, S. *Adv. Funct. Mater.* **2002,** *12,* 773. (d) Li, M.; Lebeau, B.; Mann, S. *Adv. Mater.* **2003,** *15,* 2032. (e) Viravaidya, C.; Li, M.; Mann, S. *Chem. Commun.* **2004,** 2182. (f) Rautaray, D.; Ahmad, A.; Sastry, M. *J. Am. Chem. Soc.* **2003,** *125,* 14656. (g) Rautaray, D.; Banpurkar, A.; Sainkar, S. R.; Limaye, A. V.; Pavaskar, N. R.; Ogale, S. B.; Sastry, M. *Adv. Mater.* **2003,** *15,* 1273. (h) Rautaray, D.; Sinha, K.; Shankar, S. S.; Adyanthaya, S. D.; Sastry, M. *Chem. Mater.* **2004,** *16,* 1356.
(7) (a) Lee, I.; Han, S. W.; Choi, H. J.; Kim, K. *Adv. Mater.* **2001**, *13,* 1617. (b) Rautaray, D.; Sainkar, S. R.; Sastry, M. *Langmuir* **2003,** *19,* 10095.
(8) (a) Sugawara, A.; Ishii, T.; Kato, T. *Angew. Chem., Int. Ed.* **2003,** *42,* 5299. (b) Lee, I.; Han, S. W.; Lee, S. J.; Choi, H. J.; Kim, K. *Adv. Mater.* **2002,** *14,* 1640. (c) Lu, C.; Qi, L.; Ma, J.; Cheng H.; Zhang, M.; Cao, W. *Langmuir* **2004,** *20,* 7378. (d) Volkmer, D.; Harms, M.; Gower, L.; Ziegler, A. *Angew. Chem., Int. Ed.* **2005,** *44,* 639.

crystal plates templated by sea urchin skeleton plates,[9] and porous single crystals of hexagonal vaterite prisms obtained via gelatin-mediated nanocrystal aggregation.[10] However, facile solution routes to surface-patterned $CaCO_3$ single crystals with uniform surface pores remain to be explored.

Recently, monodispersed colloidal spheres have been frequently employed as templates or porogens for the controlled synthesis of uniformly sized macroporous (pores ≥ 50 nm) inorganic materials because of their promising applications in photonics, catalysis, separation technology, and biomedical engineering.[11] Specifically, three-dimensionally ordered macroporous materials can be readily prepared by infiltration of precursors into the interstices of preformed colloidal crystal templates followed by removal of the templates with solvent extraction or calcination.[12] A great number of periodic macroporous inorganic materials including $CaCO_3$ have been synthesized by using this strategy.[11b] Recently, porous metal wires have been fabricated by electrodeposition of metals into colloidal spheres prefilled with porous membranes followed by removal of both the colloidal spheres and the membranes.[13] However, the porous products templated by colloidal particles are usually either amorphous or polycrystalline. Interestingly, Wegner et al. have managed to fabricate partially porous ZnO single crystals with a well-defined "Swiss cheese" morphology by templating of latex particles.[14] However, for the regular hexagonal prismlike ZnO single crystals, only a few surfaces exhibited the templated pores. It remains a challenge to synthesize well-defined single crystals with uniformly distributed surface pores by templating of colloidal spheres. In this work, monodispersed polymer latex particles carrying carboxylate surface groups are used as effective colloidal templates for the controlled crystallization of calcium carbonate in solution through the slow diffusion of CO_2 vapor from the decomposition of $(NH_4)_2CO_3$. After template removal, well-defined calcite single crystals exhibiting a rhombohedral morphology and uniform surface pores are obtained. In addition, the latex particles can also greatly influence the calcite morphology as a crystal growth modifier.

Experimental Section

Preparation of Monodispersed Latex Particles with $-CO_2^-$, $-SO_3^-$, $-PO_3^{2-}$, and Quaternary Ammonium Surface Functional Groups. Monodispersed P(St-MMA-AA) latex particles with $-CO_2^-$ surface functional groups were synthesized according to the reported method.[15] Namely, 120 mL of an aqueous solution, containing 0.4 g of $(NH_4)_2S_2O_8$ and 0.8 g of NH_4HCO_3 in one

funnel, and 25 mL of a monomer mixture, consisting of styrene (St)/methyl methacrylate (MMA)/acrylic acid (AA) (90:5:5 v/v/v) in another funnel, were added at the same time into a 250-mL flask. A homogeneous latex dispersion with particle diameter of $\sim$380 nm were obtained after stirring the mixture at 70 °C in N_2 atmosphere for 5 h. P(St-MMA-AA) latexes with different particle sizes were synthesized by selecting appropriate compositions of the three monomers. In a similar way, monodispersed P(St-MMA-PSPMA) latex particles carrying $-SO_3^-$ surface groups were synthesized by using potassium 3-sulfopropyl methacrylate (PSPMA) instead of acrylic acid (AA).

Moreover, a layer-by-layer electrostatic self-assembly procedure[16] was used to deposit oppositely charged polyelectrolytes on the P(St-MMA-AA) latexes ($\sim$380 nm) to tailor the surface functional groups of the latexes. Poly(diallydimethylammonium chloride) (PDDA, $M_w = 100\,000-200\,000$), poly(sodium 4-styrenesulfonate) (PSS, $M_w = 70\,000$) and sodium polyphosphate (SPP, $M = 387.86$) were purchased from Aldrich and used without further purification. Ultrathin films of $(PDDA/SPP)_2$ were deposited on the latex particles to form the outermost polyelectrolyte layer of negatively charged SPP, resulting in $-PO_3^{2-}$ surface groups. Similarly, ultrathin films of $(PDDA/PSS)_2PDDA$ were deposited on the latex particles to form the outermost polyelectrolyte layer of positively charged PDDA, resulting in quaternary ammonium surface groups.

Synthesis of $CaCO_3$−Latex Composite Particles, $CaCO_3$ Crystals with Surface Pores, and Cu_2O−Latex Composite Particles. $CaCO_3$−latex composite particles were synthesized by using the above latex particles as templates for the $CaCO_3$ crystallization. Typically, 1 mL of the prepared P(St-MMA-AA) latex dispersion (4 mg/mL) was dropped into 5 mL of 10 mM $CaCl_2$ aqueous solution under rigorous stirring. The final pH of the mixed solution was adjusted to be $\sim$10 with 10 M NaOH solution. Then the mixture was put in a closed desiccator containing a vial of $(NH_4)_2CO_3$ powders at room temperature ($\sim$22 °C) or other specified temperatures. The CO_2 vapor from the decomposition of $(NH_4)_2CO_3$ diffused into the above solution to induce $CaCO_3$ nucleation and growth. After 24 h of crystallization, the $CaCO_3$− P(St-MMA-AA) composite particles were recovered by centrifugation at 3000 rpm, thoroughly rinsed with deionized water, and dried in a vacuum at room temperature for 12 h. For the investigation of the effects of different parameters, the added volume of the latex dispersion was varied from 0.25 to 5 mL, the concentration of $CaCl_2$ aqueous solution was varied from 2 to 50 mM, and the reaction temperature was varied from 4 to 60 °C. To fabricate porous $CaCO_3$ particles, the obtained composite particles were either exposed to tetrahydrofuran (THF) at room temperature for 6 h to dissolve the latex particles or calcined at 500 °C for 4 h to burn off the latex particles. As dissolution of the copolymers was quite easy and calcination sometimes resulted in considerable crystal growth, the dissolution method was generally preferred.

In a similar way, Cu_2O−latex composite particles were prepared. Typically, 0.2 mL of 80 nm P(St-MMA-AA) latex dispersion, 0.6 mL of KOH (1 M), and 0.3 mL of $NH_3 \cdot H_2O$ (12.5 wt %) were sequentially dropped into 2 mL of aqueous $CuSO_4$ solution (0.1 M), which was followed by the addition of 0.5 mL of glucose solution (0.25 M). After the mixed solution was heated at 60 °C for 3.5 h, the precipitate was recovered by centrifugation at 3000 rpm.

Characterization. Environmental scanning electron microscopy (SEM) images were taken on a FEI Quanta 200FEG microscope at an accelerating voltage of 15 kV with the pressure in the sample chamber of 1 Torr. Transmission electron microscopy (TEM)

(9) Park, R. J.; Meldrum, F. C. *Adv. Mater.* **2002**, *14*, 1167.

(10) Zhan, J.; Lin, H.-P.; Mou, C.-Y. *Adv. Mater.* **2003**, *15*, 621.

(11) (a)Xia, Y. N.; Gates, B.; Yin, Y. D.; Lu, Y. *Adv. Mater.* **2000**, *12*, 693. (b) Yan, H.; Blanford, C. F.; Holland, B. T.; Smyrl, W. H.; Stein, A. *Chem. Mater.* **2000**, *12*, 1134. (c) Iskandar, F.; Mikrajuddin, Okuyama, K. *Nano Lett.* **2002**, *2*, 389. (d) Antonietti, M.; Berton, B.; Göltner, C.; Hentze, H.-P. *Adv. Mater.* **1998**, *10*, 154.

(12) (a) Velev, O. D.; Lenhoff, A. M. *Curr. Opin. Colloid Interface Sci.* **2000**, *5*, 56. (b) Lopez, C. *Adv. Mater.* **2003**, *15*, 1679.

(13) Li, F.; He, J.; Zhou, W. L.; Wiley, J. B. *J. Am. Chem. Soc.* **2003**, *125*, 16166.

(14) Wegner, G.; Baum, P.; Müller, M.; Norwig, J.; Landfester, K. *Macromol. Symp.* **2001**, *175*, 349.

(15) Cong, H.; Cao, W. *Langmuir* **2003**, *19*, 8177.

(16) (a) Caruso, F.; Caruso, R. A.; Möhwald, H. *Science* **1998**, *282*, 1111. (b) Khopade, A. J.; Caruso, F. *Chem. Mater.* **2004**, *16*, 2107.
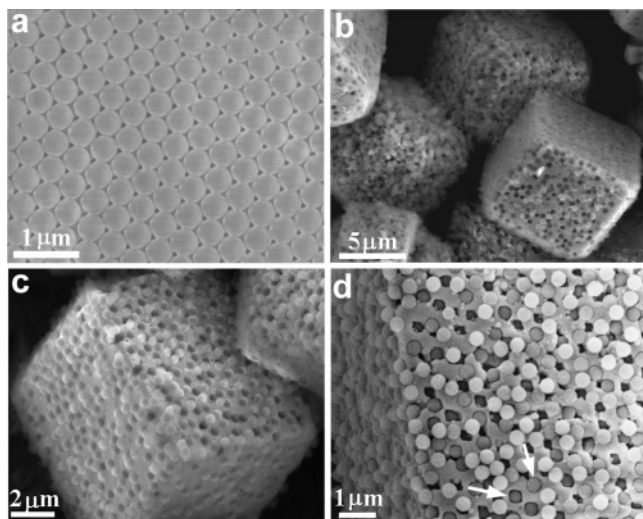
Figure 1. SEM images of P(St-MMA-AA) latex particles (a) and as-prepared CaCO₃−P(St-MMA-AA) composite particles with a latex particle size of 380 nm (b−d). Arrows in part d indicate two kinds of contours of the surface pores.

images were recorded on a JEOL JEM-200CX microscope at 200 kV. X-ray diffraction (XRD) pattern was recorded on a Rigaku Dmax-2000 X-ray diffractometer with Cu Kα radiation. Thermogravimetric analysis (TGA) was carried out on a SDT 2960 (Thermal Analysis) with the carrier gas of air at a heating rate of 10 °C min⁻¹.

Results and Discussion

Formation of CaCO₃−P(St-MMA-AA) Composite Particles and Calcite Crystals with Porous Surface. Figure 1a shows a typical SEM image of the prepared monodispersed P(St-MMA-AA) latex particles (∼380 nm in diameter), which were readily deposited on the substrate as ordered colloidal crystals. The CaCO₃−P(St-MMA-AA) composite particles obtained by templating of these latex particles are displayed in Figure 1b−d. As shown in Figure 1b, the particles show a rhombohedral morphology characteristic of single crystals of calcite with a crystal size ∼8 μm on average, which is relatively smaller than the control samples obtained without latex particles (∼20 μm). Enlarged images shown in Figure 1c,d suggest that all the surfaces of the rhombohedral particles exhibit embedded latex particles and hollow holes together with some latex particles departed from the host pores and attached to the outermost surface. Apparently, there are two typical kinds of pore contours (i.e., round and square), indicating that both the shape of the colloidal templates and the crystalline nature of calcite play a role in determining the final morphology of the latex-embedded surface. The X-ray diffraction (XRD) pattern of the composite particles (Figure 2a), which was measured from the sample prepared by dispersion of the particles in water followed by careful deposition of a thin layer on the glass substrate, shows reflections characteristic of calcite with the (104) reflection considerably intensified compared with the standard diffraction intensities of calcite (JCPDS 47-1743). This result can be rationalized by considering that the micrometer-sized crystals predominantly adopted a rhombohedral morphology and they tended to lie on their {104} planes. It strongly indicates that observed rhombo-
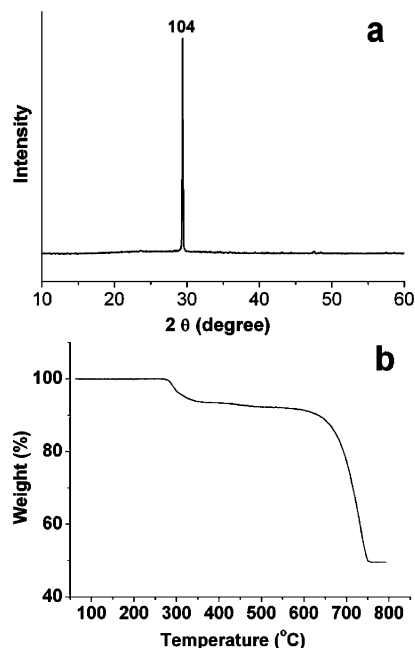
Figure 2. XRD pattern (a) and TGA curve (b) of CaCO₃−P(St-MMA-AA) composite particles.
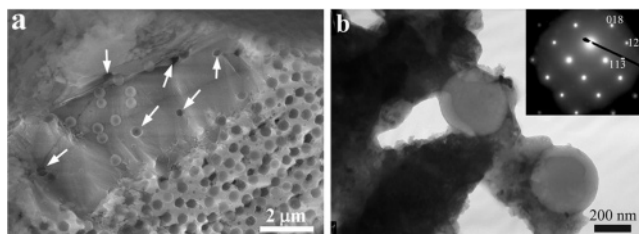
Figure 3. SEM (a) and TEM (b) images of partially broken CaCO₃−P(St-MMA-AA) composite particles with a latex particle size of 380 nm. Arrows in panel a indicate inner pores templated by the latex particles incorporated inside the composite particles. The inset in panel b shows the related SAED pattern.

hedral inorganic−organic composite particles were actually {104}-bound single crystals of calcite containing incorporated latex particles. The corresponding thermogravimetric analysis (TGA) curve of the composite particles (Figure 2b) shows that the incorporated latex particles started to be burned off around 280 °C and the calcite crystals started to decompose ∼660 °C. Furthermore, it was estimated that about 8.7 wt % (corresponding to ∼20 vol %) of the P(St-MMA-AA) latex particles were incorporated in the composites.

To elucidate whether the latex particles were incorporated inside the crystals, the as-prepared composite particles were ground to obtain broken particles. The image of a partially crushed composite particle shown in Figure 3a reveals that only a few latex particles were entrapped in the inner part of the crystals, which is in contrast to the large number of latex particles densely distributed on the surface layer of the crystals. A thin section of the composite particle is presented in Figure 3b, which shows the incorporation of latex particles in calcite crystals. The corresponding selected area electron diffraction (SAED) pattern exhibits clear spots associated with the [11 8̄ 1] zone axis of the rhombohedral calcite, confirming that the entire crystal incorporating latex particles is actually a single crystal of calcite.
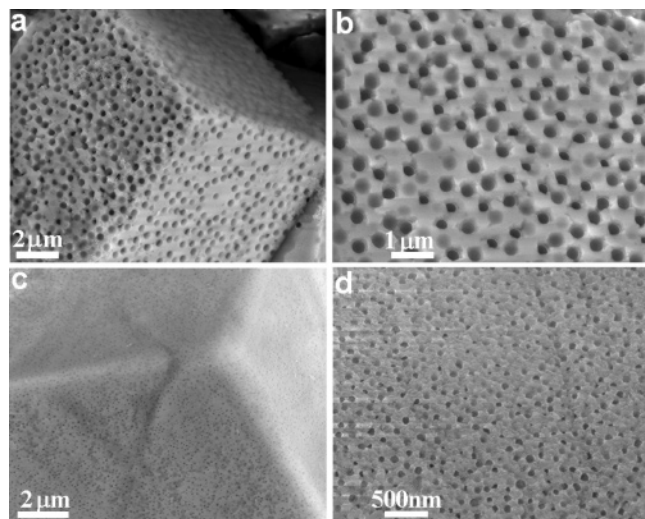
Figure 4. SEM images of CaCO$_3$ particles with porous surface obtained by templating and THF extraction of P(St-MMA-AA) latex particles with different sizes: (a,b) 380 nm, (c,d) 80 nm.

Surface-patterned single crystals of calcite showing a well-preserved rhombohedral morphology and evenly distributed surface pores were readily prepared by exposure of the CaCO$_3$−P(St-MMA-AA) composite particles to tetrahydrofuran (THF) to dissolve the latex particles or calcination at 500 °C to burn off the latex particles. Figure 4 presents typical SEM images of the porous calcite crystals obtained by templating of latex particles with different sizes followed by THF extraction. As shown in Figure 4a,b, the evenly distributed surface pores, which apparently show contours between spherical and rhombohedral, were imprinted by 380-nm latex particles with somewhat different embedding depths. When monodispersed P(St-MMA-AA) latex particles with a size ∼80 nm were used as the templates, rhombohedral single crystals of calcite showing uniform surface pores templated by the latex particles can be produced in a similar way (Figure 4c,d). This result suggests that the surface pore size of the porous calcite single can be well-adjusted through introduction of latex particles with varied sizes, since colloidal chemical approaches have been well-established to synthesize monodispersed polymer latex particles with tailored sizes. Compared with the previously reported porous ZnO single crystals with only a few surfaces showing latex-templated pores,[14] the current calcite single crystals show evenly distributed surface pores, which could be related to the controlled precipitation process of CaCO$_3$ from the slow diffusion of CO$_2$.

Growth Process of the CaCO$_3$−P(St-MMA-AA) Composite Particles. To obtain more information on the formation of the final CaCO$_3$−P(St-MMA-AA) composite particles, we collected the crystal product formed at an early stage of CaCO$_3$ crystallization. The SEM image of the product obtained at 1 h of crystallization (Figure 5a) suggests that nearly spherical or elongated particles with sizes slightly larger than 380 nm, i.e., the latex particle size, were formed, indicating that CaCO$_3$ crystals preferentially nucleated on the latex particles and grew into CaCO$_3$-coated latex particles. This result can be rationalized by considering that the polymer latex particles carried carboxylate surface groups that interacted strongly with Ca^{2+} ions as well as CaCO$_3$
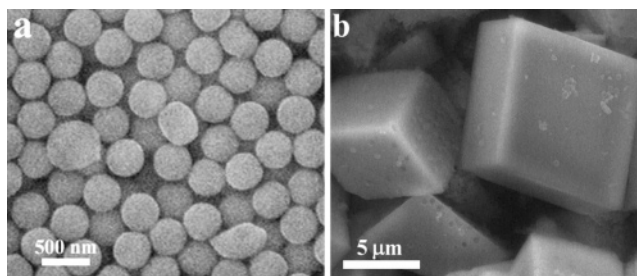
Figure 5. (a) SEM image of early CaCO$_3$−P(St-MMA-AA) composite particles obtained after 1 h of CaCO$_3$ crystallization with 380 nm latex particles. (b) SEM image of the calcite crystals obtained after the early composite particles shown in panel a were used as crystal nuclei for further growth in CaCl$_2$ solution without latexes.

crystal surfaces, which may induce the preferential calcite nucleation.[6a,8c] It is speculated that after the initial formation of the calcite-coated latex particles, the subsequent crystal growth occurred mainly through continuous addition of Ca^{2+} ions and CO$_3^{2-}$ ions with latex particles occasionally attached, leading to the formation of rhombohedral single crystals of calcite with a few latex particles entrapped inside the crystals. In the final stage of crystal growth, the Ca^{2+} ion concentration in the solution was decreased considerably, and hence the free latex particles were simultaneously attached to the surfaces of rhombohedral calcite crystals accompanying further growth of calcite crystals, resulting in the uniform embedding of many latex particles in the surface layer of the calcite rhombohedrons. Our further SEM observations of the crystallizing calcite crystals after being crushed manually and washed with THF also showed that only a quite small amount of latex particles was incorporated inside the particles, indicating a sudden embedding of latex particles into the surface layer of the crystallizing calcite particles in the final stage. In short, the formation of the composite particles consisting of single crystals of calcite may be explained by the proposed three-step mechanism, i.e., initial calcite nucleation on latex particles, intermediate calcite crystal growth, and final embedding of latex particles. To support the proposed formation mechanism, the early composite particles shown in Figure 5a were put into CaCl$_2$ solution without latexes and then subject to further growth. As expected, most of the obtained rhombohedral crystals show smooth surface instead of porous surface (Figure 5b), testifying to a further growth process. It is also noted that a few pores are occasionally observed on the crystal surface, which could be attributed to the involvment of a few bare latex particles in the early composite particles during the separation process by centrifugation.

It may be argued that the intermediate growth process might proceed by the fusion of the growing latex-containing crystallites through an oriented attachment mechanism, which was initially put forward by Penn and Banfield[17] and subsequently applied for the interpretation of the anisotropic growth of a variety of 1D nanostructures.[18] However, such

(17) (a) Penn, R. L.; Banfield, J. F. *Science* **1998**, *281*, 969. (b) Banfield, J. F.; Welch, S. A.; Zhang, H.; Ebert, T. T.; Penn, R. L. *Science* **2000**, *289*, 751.

(18) (a) Pacholski, C.; Kornowski, A.; Weller, H. *Angew. Chem., Int. Ed.* **2002**, *41*, 1188. (b) Cho, K. S.; Talapin, D. V.; Gaschler, W.; Murray, C. B. *J. Am. Chem. Soc.* **2005**, *127*, 7140.
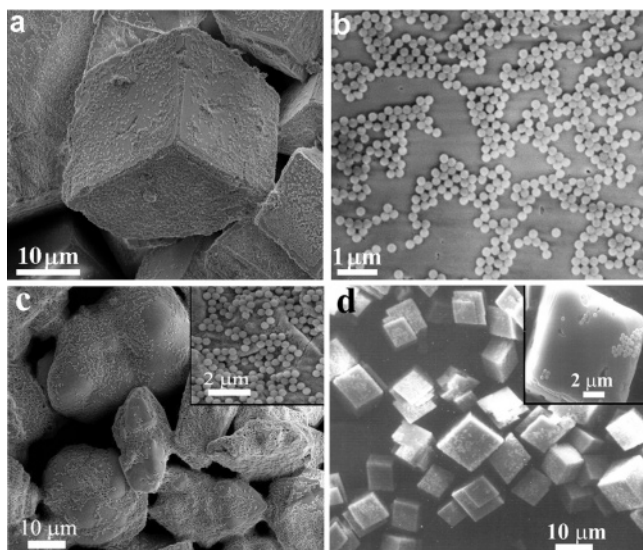
Figure 6. SEM images of latex-particle-attached CaCO₃ particles obtained in the presence of latex particles carrying different surface functional groups: (a, b) $-SO_3^-$, (c) $-PO_3^{2-}$, and (d) quaternary ammonium.

Figure 7. SEM images of CaCO₃ particles with porous surface obtained by templating of 380-nm P(St-MMA-AA) latex particles with different volumes of added latex dispersion: (a) 0.25 mL, (b–d) 5 mL.

a mechanism is usually applicable for the oriented attachment of very small nanocrystals rather than relatively large particles (e.g., >100 nm); hence, this possibility seems quite low in the current situation. Moreover, our preliminary experiments showed that rhombohedral crystals formed very quickly after the nucleation of calcite on some latex particles, leading to coexistence of latex-containing rhombohedral crystals and many nearly bare latex particles. Therefore, we believe that the intermediate growth process most probably took place through the further growth on latex-containing calcite nuclei with bare latex particles incorporated occasionally. However, it remained unclear why the nucleation occurred just on a few latex particles with a large number of particles only barely covered. A possibility is that the surface charge distribution of the latex particles may have a certain degree of inhomogeneity despite the homogeneity in particle size. Another possibility is that the process of CO₂ diffusion into the dispersion could bring about a somewhat inhomogeneous calcite nucleation on latex particles.

Effect of Surface Functional Groups of the Latex Particles. It is supposed that carboxylate surface groups of the P(St-MMA-AA) latex particles may play a key role in the formation of the CaCO₃−P(St-MMA-AA) composite particles. There is a possibility that the embedding of the negatively charged latex particles into the surface layer of the calcite particles may be simply attributed to the electrostatic interaction between the anionic $-COO^-$ groups and the cationic Ca^{2+} ions. In this regard, CaCO₃ crystallization has been also carried out in the presence of latex particles carrying different surface functional groups, and the obtained results are shown in Figure 6. If the latex particles carried $-SO_3^-$ surface groups, which had a relatively weak interaction with Ca^{2+} ions and CaCO₃ crystal surface, the obtained product showed rhombohedral calcite crystals with latex particles attached on the smooth crystal surfaces and no obvious embedding of the latex particles was observed (Figure 6a,b). When the latex particles containing $-PO_3^{2-}$ surface groups were used as templates, the product showed irregular morphologies, probably due to the inhibition effect
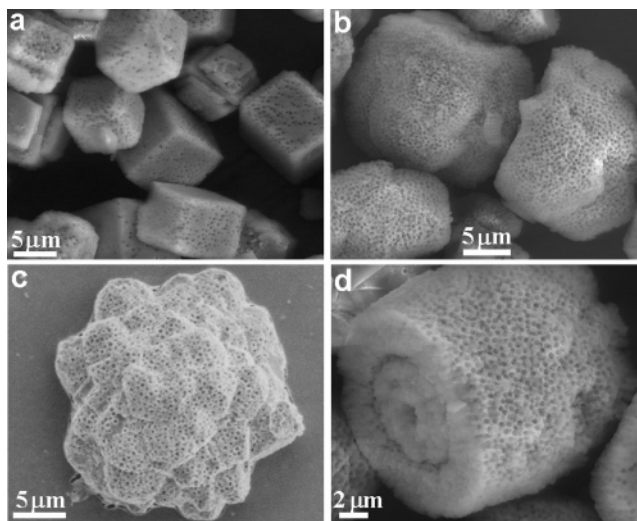
of $-PO_3^{2-}$ groups on the CaCO₃ crystallization (Figure 6c). Meanwhile, the latex particles were just attached on the crystal surfaces without obvious embedding of the latex particles. On the other hand, if the latex particles contained cationic quaternary ammonium surface groups, only very few latex particles were adsorbed on the crystal surface while the crystals retained a rhombohedral morphology. These results suggest that the electrostatic interaction between the surface functional groups and the Ca^{2+} ions does not play a key role in the embedding of the latex particles into calcite crystals, although it may favor the adsorption of the latex particles onto the crystal surface. Instead, the specific interaction between the anionic $-COO^-$ groups and the Ca^{2+} ions or the calcite crystal surface may be largely contributed to the formation of the latex-particle-incorporated calcite crystals, confirming the importance of the surface groups of the colloidal templates.

Effect of Latex Particle Concentration and CaCl₂ Concentration. It has been found that the concentration of the latex dispersion can also exert great influence on the exterior morphology of porous calcite crystals. As shown in Figure 7a, at a fixed CaCl₂ solution concentration of 10 mM, rhombohedral calcite crystals with somewhat lower density of surface pores were produced at a P(St-MMA-AA) latex concentration smaller than the standard concentration (i.e., 1 mL of the original latex dispersion was added to 5 mL of CaCl₂ solution). In contrast, porous calcite crystals with higher density of surface pores, which exhibited irregular and complex morphologies, were obtained at a higher latex concentration (Figure 7b–d). This result indicates that a relatively high concentration of latex particles may act as both colloidal templates and crystal growth modifiers to influence the crystallization of calcium carbonate, which could be further used for the controlled synthesis of porous calcite crystals with hierarchical architectures. The synthesis was also conducted at the standard latex concentration to examine the effect of the reactant concentration. At a lower CaCl₂ solution concentration (2 mM), the obtained CaCO₃ particles exhibited an irregular morphology with many latex particles incorporated into the surface layer (Figure 8a),
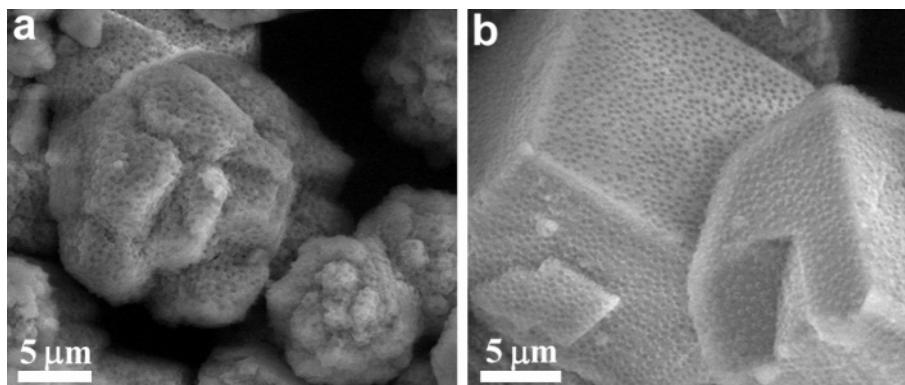
Figure 8. SEM images of $CaCO_3$−P(St-MMA-AA) composite particles obtained by templating of 380-nm P(St-MMA-AA) latex particles with different $CaCl_2$ concentrations: (a) 2 mM, (b) 50 mM.
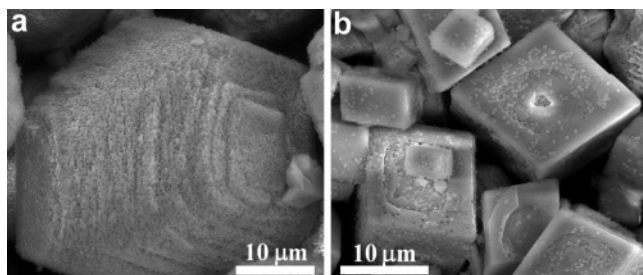
Figure 9. SEM images of $CaCO_3$ products obtained in the presence of 380-nm P(St-MMA-AA) latex particles at different temperatures: (a) 4 °C, (b) 60 °C.

Figure 10. SEM images of octahedral Cu_2O−P(St-MMA-AA) composite particles by templating of 80 nm P(St-MMA-AA) latex particles.

somewhat similar to the case of synthesis at an increasing latex particle concentration. When the concentration of the $CaCl_2$ solution was increased to 50 mM, well-faceted calcite crystals showing a roughly rhombohedral morphology and latex-particle-incorporated surface were obtained (Figure 8b). These results suggest that a higher ratio of the latex concentration with respect to the $CaCl_2$ solution concentration would lead to the formation of calcite crystals with irregular morphologies, possibly due to the intensified role of latexes as the crystal growth modifiers.

Effect of Reaction Temperature. Till now, the $CaCO_3$ crystallization in the presence of latex particles was always carried out at room temperature (∼22 °C). The effect of the reaction temperature on the $CaCO_3$ crystallization was also investigated, and the obtained results are presented in Figure 9. The calcite crystals obtained at a lower temperature (4 °C) usually did not show a regularly rhombohedral morphology, while latex particles were densely incorporated in the surface layer of the crystals (Figure 9a). This might be attributed to the enhanced inhibition effect of the latex particles, since the $CaCO_3$ crystallization was slowed at lower temperature due to the slower $(NH_4)_2CO_3$ decomposition and CO_2 diffusion, so the latex particles would access the crystallizing particles more easily. If the temperature was increased up to 60 °C, rhombohedral calcite crystals showing poisoned {104} surfaces were produced while much fewer latex particles were incorporated in the surface layer of the crystals (Figure 9b). Since a higher temperature would result in a faster $CaCO_3$ crystallization process, rhombohedral calcite crystals with imperfect surface would result from the very quick crystallization process. Meanwhile, it could be more difficult to simultaneously incorporate many latex particles into the surface layer of the calcite crystals at the
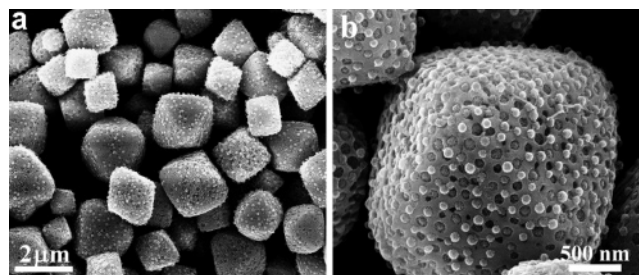
higher temperature, leading to fewer incorporated latex particles, which provides further support for the proposed three-step growth mechanism for the latex-particle-loaded single crystals of calcite.

Synthesis of Octahedral Cu_2O−P(St-MMA-AA) Composite Particles. It is expected that this synthesis strategy may be extended to the synthesis of regularly shaped composite particles consisting of single crystals of other inorganic materials. To illustrate, octahedral Cu_2O−P(St-MMA-AA) composite particles have been successfully synthesized by templating of 80 nm P(St-MMA-AA) latex particles by using this strategy (Figure 10). The octahedral morphology is typical of Cu_2O crystals with a cubic structure, suggesting that the obtained composite particles consist of Cu_2O single crystals with latex particles embedded in the surface layer, very similar to the case of rhombohedral $CaCO_3$−P(St-MMA-AA) composite particles.

Conclusions

In summary, monodispersed copolymer latex particles functionalized by surface carboxylate groups were successfully used as effective colloidal templates for the synthesis of well-defined calcite single crystals with latex particles evenly embedded in the surface layer and a few incorporated in the interiors. Rhombohedral, single crystals of calcite exhibiting uniform, submicrometer-sized surface pores were readily fabricated by subsequent template removal. It has been revealed that the carboxylate surface groups of the latex particles played a key role in the embedding of the latex particles into calcite crystals, and a higher ratio of the latex concentration with respect to the $CaCl_2$ concentration would lead to the formation of calcite crystals with irregular morphologies. A three-step mechanism has been proposed

for the formation of the latex particle-embedded single crystals of calcite, i.e., initial calcite nucleation on latex particles, intermediate calcite crystal growth, and final embedding of latex particles. This synthesis strategy is potentially extendable to other inorganic crystal systems, and it may represent a novel route to achieve the direct surface patterning of single crystals on the submicrometer scale. The effects of surface-functionalized organic templates on the formation of surface-patterned single crystals of calcite may provide new insights into the formation of calcite single crystals with complex morphologies in biomineralization.

CM0513029